Non-Invasive Prediction of Fracture Risk Due to Metastatic Skeletal Defects

Brian D. Snyder, MD, PhD, John A. Hipp, PhD, Ara Nazarian, MSc

Excerpted from the 2004 Ann Doner Vaughn Kappa Delta Award Paper

Background

This collaborative effort between clinicians and engineers began as a request by clinicians to provide more reliable methods for predicting the risk of fracture due to metastatic defects in the bone of their patients. These requests were addressed by several years of NIH funded research into the structural consequences of metastatic defects in bone. This early work showed that sophisticated computer models could be used to predict the load bearing capacity of a bone with a simulated defect. It was recognized that complicated computer models were not practical in routine clinical applications. This led to investigations into the application of relatively simple engineering tools to solving the clinical problem. These investigations began with the basic science of applying simple engineering theory to predicting the structural consequences of defects in bone. These basic science studies validated the basic hypotheses and led to application of the methods in two clinical trials, one with benign bone defects in children and the other one with metastatic defects in patients with breast cancer. In these clinical studies, the technology has proven much better at predicting the structural effects of bone defects than methods that are now commonly used in clinical practice in these clinical trials. We therefore present a portion of our work as it relates to fracture risk prediction in metastatic skeletal defects.

Introduction

The skeleton is the third most common site of metastatic cancer after the liver and the lung, and one third to half of all cancers metastasize to bone.[1] As a result of new and aggressive treatment, cancer patients are living longer but skeletal metastases continue to be a feared complication since at sites of bone involvement patients can experience intractable pain, fracture after minimal trauma, become paralyzed from spinal cord compression and develop hypercalcaemia. One of the key components of successful clinical management is the prevention of pathologic fractures and minimizing the destruction of bone. While much has been learned about the mechanisms of metastatic spread of cancer to bone, little headway has been made in establishing reliable guidelines for estimating fracture risk associated with skeletal metastases or monitoring the response of a specific bone lesion to treatment. Although guidelines have been described, most clinicians make subjective assessments regarding fracture risk and treatment response based on plain radiographs using methods now recognized to be inaccurate. The prevention of fractures due to skeletal metastasis depends on objective criteria for evaluating changes in the bone structural properties that reflect the interaction of the tumor with the host bone.

Systemic treatment with cytotoxic agents, hormone manipulation, bisphosphonates or local treatment with radiation and/or surgical stabilization constitutes the range of therapies available to cancer patients with skeletal metastases.[4-14] Identifying which of these treatments is optimal for a particular patient is controversial,[15] in part because there are no proven objective methods for evaluating a patient's response to treatment. Biochemical markers have been used to assess the extent of metastatic spread to the skeleton and to monitor the efficacy of drugs used to treat symptoms of skeletal metastases, however these serum assays do not identify whether fracture risk is increasing or decreasing for a specific skeletal lesion. Magnetic Resonance Imaging (MRI) has been used to assess changes in tumor volume as a measure of response to treatment, but MRI cannot readily assess the healing response of the host bone or the associated fracture risk.

Osteoclasts and osteoblasts change the host bone structure in response to local and systemic cytokines, growth factors and hormones secreted by tumor cells. If changes in bone structure reflect the interaction of the tumor with the bone, then the bone structural properties (which reflect the combined effect of bone material properties and bone cross-sectional geometry) can be used to monitor the deterioration of the bone structure by progressive tumor growth. It follows that image based methods that measure both bone mineral density and whole bone geometry can be used to monitor whether a specific lesion has weakened the bone sufficiently such that pathological fracture is imminent. Our hypothesis is that changes in bone structural properties as a result of tumor induced osteolysis determine the fracture risk in patients with skeletal metastases. Our goal was to develop an imaged based

Brian D. Snyder, MD, PhD is an Assistant Professor of Orthopaedic Surgery, Harvard Medical School and Director of the Orthopedic Biomechanics Laboratory, Beth Israel Deaconess Medical Center, Harvard Medical School.

John Hipp, PhD is Director of the Spine Research Laboratory, Baylor College of Medicine, Houston, TX.

Ara Nazarian MS is a graduate student at the Swiss Federal Institute of Technology, Zurich, Switzerland.

Please Address Correspondence to:

Brian Snyder, MD
Beth Israel Deaconess Medical Center
Orthopedic Biomechanics Laboratory
330 Brookline Ave., RN115
Boston, MA 02215
Phone No: (617) 667-2940
Fax No: (617) 667-7175
Email: bsnyder@bidmc.harvard.edu

clinical tool to monitor the fracture risk associated with individual lesions in patients with skeletal metastases so as to optimize treatment and to monitor a patient's response to treatment.

The Clinical Problem

There are over a million new cancer cases annually in the U.S.[16] Breast, prostate and lung carcinomas have a propensity to metastasize to bone. Almost all patients with myeloma have extensive bone destruction, and nearly 80% of these patients present with complaints of bone pain. The breast is the most common site of cancer in women, afflicting one in nine women over the age of 30. Among breast cancer patients, the skeleton is the most common site of metastases. With the prolonged survival of breast cancer patients, the incidence of symptomatic bone metastases has increased. Of breast cancer patients with skeletal metastases 25-40% will require radiotherapy for bone pain, 30% will develop hypercalcaemia and 17-50% will sustain a vertebral fracture.[17,18] While the incidence of skeletal complications is lower in myeloma patients than breast cancer patients, new vertebral fractures occur in 15-30% of myeloma patients, and fractures of the appendicular skeleton occur in 5-10% of myeloma patients annually. Assessing the effects of these lesions on bone fracture risk has become an important clinical problem since pathologic fractures profoundly affect patient function and mobility.

The dilemma for the orthopaedist who is often consulted in the management of these patients is to decide whether the defect has weakened the bone sufficiently such that pathological fracture is imminent. When pathologic fractures occur in the femur, humerus or periacetabular pelvis, approximately 90% of patients require surgical intervention to relieve pain and restore function and mobility. Based on retrospective clinical studies, previous investigators have considered pain, geometry, anatomic site, lesion type, and activity level to be predictors of fracture risk for metastatic tumors of the appendicular skeleton.[2,24-29] While pain is a common presenting symptom, it is not present in all patients with skeletal metastases and is therefore not a reliable indicator of fracture risk or response to treatment. Since skeletal tumors are initially diagnosed from evaluation of plain radiographs, several investigators have attempted to estimate the load-bearing capacity of a bone with a lytic defect by measuring the geometry of the defect on the radiograph. Two guidelines frequently cited are: 1) that a defect greater than 2.5 cm in diameter should be considered at risk of fracture; and 2) that greater than 50% cortical destruction is an indication for prophylactic stabilization.[2,24,30-32] These guidelines arise from several retrospective clinical studies conducted in adults with skeletal metastases, however neither guideline has been confirmed experimentally in-vitro or evaluated prospectively in-vivo.[33]

Based on the available literature, radiographic guidelines that use some measure of defect geometry allow for probabilities of clinical errors up to 42%, with potentially unnecessary skeletal stabilization in up to 67% of patients.[33] As a result, optimal treatment for skeletal metastases remains a controversial topic,[15] in part because there are no objective methods for evaluating patient response to different treatments. Most importantly, a reliable method to quantify the response of bone to treatment for skeletal metastases could be a valuable tool in the management of the thousands of patients treated each day in the United States.

Experimental Validation

Preliminary Work

We initially conducted a series of ex-vivo investigations that logically built upon one another to validate the algorithm for predicting the failure load and then demonstrated in-vivo that image-based structural analysis was an improvement over current methods for predicting pathologic fracture in patients with osteolytic tumors.[36,38] Using trabecular core samples from whale vertebrae, we demonstrated that the structural rigidity (calculated using composite beam theory from non-invasive imaging methods) of the weakest cross-section of a trabecular bone with a lytic defect highly correlates with the load capacity of the bone and correlates better than material or geometric properties alone.

Table 1. Coefficients of determination (r^2) for linear regression between structural properties measured by QCT and yield load in different mechanical testing modes. The structural rigidity based on constant strain failure theory correlated best, while the ratio of hole diameter to bone diameter (current clinical practice) or geometry alone correlated much worse. (A = area, I = bending moment of inertia, J = polar moment of inertia, E = modulus of elasticity, G = shear modulus)

Property	Failure Theory	Bending	Torsion	Tension
Hole Dia Ratio (d/D)	Clinical/x-ray	0.32	0.22	0.25
Material: Density	Strength Based	0.55	0.81	0.72
Geometry: A, I_{min}, J	Const. Stress	0.33	0.40	0.38
Structure/ QCT:A,EI_{min},GJ	**Const. Strain**	**0.92**	**0.89**	**0.95**
A, I, J	Strain Energy	0.86	0.90	0.89

We subsequently tested whether structural rigidity measured using CT, DXA, and MRI could also predict the yield loads in whale bone trabecular specimens with simulated lytic defects. These tests were completed to determine if other common imaging modalities could also be used to non-invasively measure structural rigidities. We found that cross-sectional structural properties calculated from CT, DXA, and MRI accurately predicted the failure of trabecular bone with and without simulated circular and slotted lytic defects.

Table 2. Coefficients of determination (r^2) between structural rigidity calculated using different imaging modalities and yield loads in different mechanical testing modes. The current clinical guideline is also represented by the ratio of defect diameter to whole bone diameter (d/D). The results clearly indicate that structural rigidity correlates better than the current clinical guideline based on defect size. For CT, DXA and MRI, correlation was between structural rigidity (EA for tension, EI_{min} for bending, and GJ for torsion) and yield load. For the current clinical guideline, the ratio d/D was correlated directly to the yield load.

Test Mode	CT	DXA	MRI	d/D
Tension	**0.95**	0.93	0.92	**0.25**
Bending	**0.91**	0.84	0.86	**0.32**
Torsion	**0.91**	0.92	0.85	**0.22**

Quantifying the size of a defect in a bone structure was not adequate to predict the failure of bone, because structural behavior depends on both the cross-sectional geometry and material properties of the bone. In comparison to current clinical guidelines, structural rigidity was demonstrated to be a better predictor of failure.

Non-invasive Imaging Predicts Failure Load of Whole Bones with Simulated Osteolytic Defects

After demonstrating that structural rigidity calculated from multiple non-invasive imaging methods accurately predicts failure load of regularly shaped bones with simulated lytic defects, we investigated whether similar methods could be used in complex structure with irregularly shaped geometry such as human spine and proximal femur. The hip and spine are the most common sites of bone metastasis in both breast and prostate cancer, and results of the study are relevant to the clinical management of patients with metastasis to the hip and/or spine. Our previous work showed that the load capacity for each cross-section through the bone depends on its corresponding structural rigidity. Structural rigidity is the product of a *material* property (*i.e.* modulus of elasticity, E, or shear modulus, G) and a *geometric* property (*i.e.* area, A; moment of inertia, I; or polar moment of inertia, J) which describe how the material is arranged in space relative to a bending or twisting axis. The axial (EA), bending (EI) and torsional (GJ) rigidity for each transaxial cross-section through the bone integrates the site, size and location of the defect and the material and geometric properties of the host bone. We therefore investigated the use of DXA, CT, and MRI as non-invasive tools for measuring the structural properties and for predicting the failure load of whole bones with simulated lytic defects of intermediate size.

Spine

Thirty-five elderly (mean age 72 yrs., range 37-102 yrs.) human fresh frozen cadaver spines were segmented into 3-body functional spinal units (FSU) at the thoracic and lumbar levels. Lytic defects, comprising 30% of the cross-sectional area, were created with a burr in the middle vertebral body. The location of the defect was randomly assigned among at three different locations (See Figure 1). The spines were non-invasively imaged

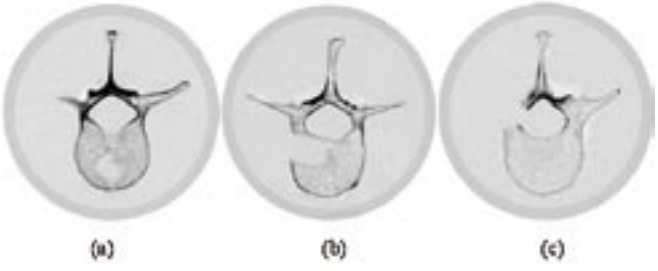

Figure 1. QCT transverse images of vertebrae with simulated lytic defects comprising approximately 30% of the cross-sectional area. a) contained defect in the anterior region of the vertebral body centrum, b) uncontained defect in the postero-lateral region of the vertebral body centrum, and c) an uncontained region in the posterior third of the vertebrae destroying the costovertebral joint in thoracic vertebrae or pedicle in lumbar vertebrae.

following similar protocols described in the previous studies, using DXA ,CT and MRI. For both QCT and MRI, a power law relationship described by Rice *et al.* [37] was used for trabecular bone , and a linear relationship described by Snyder *et al.* was used for cortical bone.[38] The axial and bending rigidities of each cross section were calculated by summing the rigidity of each pixel about the modulus-weighted neutral axis.

After imaging, the spines were mechanically tested to failure using a custom-designed spine-testing machine. The testing machine loaded the spine asymmetrically using hydraulic

actuators to create axial compression combined with forward flexion. The compression failure load (F_m) and other components of forces and moments were recorded with a multi-axial load cell connected to the spine. For combined load of bending and compression, beam theory predicts that strain (ε) is:

$$\varepsilon = F_p/AE + Mc/EI,$$

where, F_p is the compression force, M is the bending moment, c is the distance from the neutral axis, AE is the axial rigidity, and EI is the bending rigidity. AE and EI were calculated from the non-invasive imaging methods described previously, and *c* can be similarly measured from the images. The bending moment (M) can be derived empirically as a function of the applied load. Thus, using bone failure strain of 1%,[39] the compression load (F_p) at which the spine will fracture was predicted using the non-invasive imaging methods.

Although the relative cross-sectional area of the defect was constant, there was a 59% coefficient of variation in measured failure loads. Hence, the relative defect size does not account for the variation in failure loads of vertebrae with lytic defects of intermediate size, and so is not a good predictor of fracture risk. For DXA measurement, correlations between the measured failure load with density and axial rigidity were significantly better than those with bending rigidity and calculated failure load using composite beam theory (See Table 3). For CT measurement, correlations between measured failure load and material or cross-sectional structural properties were not significantly different ($p>0.25$). Finally, the concordance correlation (r_c) between the QCT-predicted failure load (F_p) and the measured failure load (F_f) was 0.74 (See Figure 2). This result demonstrates that theoretically predicted failure load, calculated from CT-measured structural properties, corresponded closely on a one-to-one basis to the experimentally measured failure load for human vertebrae with lytic defects. Therefore, this prospective measure should allow clinicians to more reliably predict pathologic fracture of structurally compromised vertebrae so that appropriate treatments can be administered.

	Density (_, g/cm³)	Axial Rigidity (EA, N)	Flexural Rigidity (EI, Nm²)	Predicted Load (Fp, N)
DXA	0.72	0.71	0.35	0.44
CT	0.42	0.51	0.63	0.69
MRI	0.08	0.42	0.56	0.40

Table 3. Coefficients of determination (r^2) for linear regression between measured failure load (Fm) of human vertebrae with simulated lytic defects and various measurements from non-invasive imaging methods.

Femur

To study the proximal femur, clinically representative

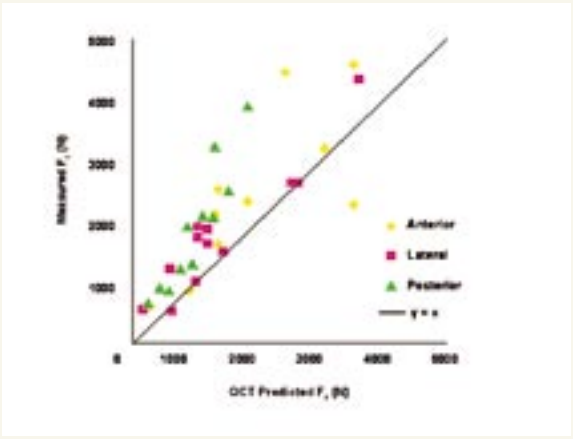

Figure 2. CT predicted failure load vs. measured failure load (concordance rc=0.74). The theoretical prediction based on composite beam theory.

ellipsoidal defects (20-50% cross-sectional area) were created at the intertrochanteric region of ten adult cadaver femurs using a burr directed under fluoroscopic guidance. Specimens were then scanned using CT to determine equivalent bone density. The fracture force for an applied load configuration simulating single legged stance (See Figure 3) was measured experimentally and compared to the predicted failure load using a simplified curved beam, plane stress model of the femur that assumed failure to occur at the weakest cross-section through the bone determined from CT-based structural analysis. The failure load was calculated for combined axial compression and bending, based on axial and bending rigidities calculated from the CT data and a strain based failure criterion independent of density (tensile failure strain of 0.8% and compressive failure strain of 1%) (See Figure 4).[39] The average of the calculated failure loads using tensile and compressive failure strains was not different from the measured failure load (predicted = 6.17 ± 1.82 kN vs. measured = 7.14 ± 1.61kN; t=1.34, p=0.20) and came close to predicting the actual measured fracture load (absolute error = 2.1±1.2 kN). The results of this study demonstrate that for the simplified load case of single legged stance, the location of the minimum predicted failure load calculated using a plane stress, curved beam, composite material model of the femur and a compressive failure strain of 1% correctly identified the site of actual fracture. The best estimate of the actual fracture load at that site was given by the average of the calculated failure loads for the model using a tensile failure strain of 0.8% and compressive failure strain of 1%.

Figure 3. Exp. set up for single Legged Stance(load applied to femoral head). Torsional spring provides varus/valgus resistance moment at the knee. 6DOF load cell measures resultant forces and moments.

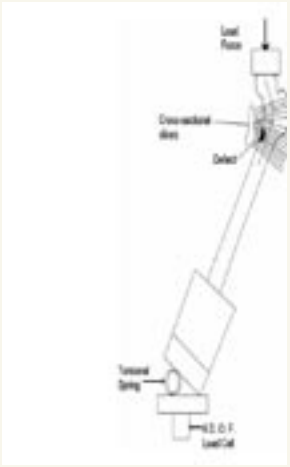

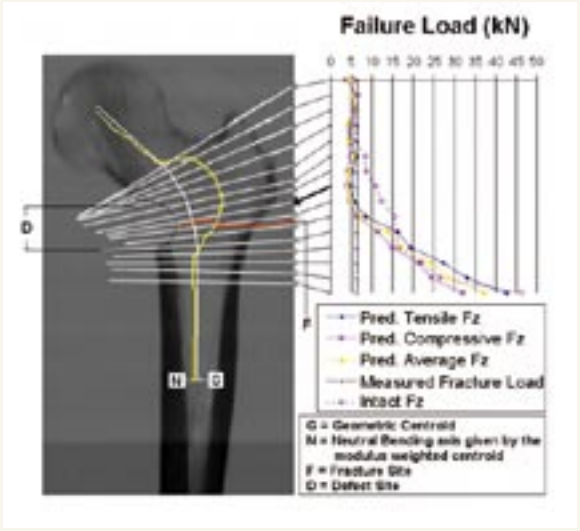

Figure 4. Predicted failure load for tensile and compressive failure strains for transaxial cross-sections perpendicular to the trajectory of geometric centroid (white). Modulus weighted centroid illustrated in yellow. Fracture occurred at the cross-section of the minimum predicted compressive failure load (red).

Validation of Density-Modulus Relationships for Metastatic Bone Tissue

Our CT based structural analysis for predicting fracture through a skeletal metastasis is based on the assumption that all bone (normal or pathologic) follows the same constitutive relationships established for rigid porous foams, i.e. the strength (σY) and modulus of elasticity (E) of bone depend on both the bone tissue density (ρ_{tiss}) and the bone volume fraction (Vv_b) squared:[40]

$$\sigma Y,\ E = a \cdot \rho_{tiss} \cdot (Vv_b)^2 + b$$

The ρ_{tiss} accounts for changes in tissue mineralization, and the Vv_b accounts for changes in trabecular morphology. To the best of our knowledge, this hypothesis has never been validated for metastatic cancer bone tissue. Therefore, it was our objective to establish that the mechanical properties of metastatic cancer bone tissue were governed by the power law functions that work for normal, [with the minimum Vv_b predicted the mechanical properties of the specimen better than the average Vv_b for the entire specimen.]

With IRB approval, 15 patients underwent excisional biopsy of prostate, breast, lung, ovarian or colon cancer metastatic to bone at surgery or necropsy. Lytic or osteoblastic metastases were identified from biplanar radiographs. Of these

specimens, 11 (7 male, 4 female, 70 ±15 years) were of adequate size to undergo specimen preparation for mechanical testing. A pathologist confirmed the presence of metastatic cancer in each cancer specimen by histology. In addition, 18 normal cadaveric femurs (13 male, 5 female, 58 ± 21 years) were obtained. After freezing, 57 trabecular cores with a 2:1 aspect ratio were created (31 cancer, 26 non-cancer) The ρ_{tiss} of each specimen was measured using a pycnometer (Quantachrome, Boynton Beach, FL). The average Vv_b for the entire specimen and the Vv_b for each of 10 equally divided transaxial sub-regions were determined from thresholded μCT images (Scanco Medical AG, Bassersdorf, Switzerland). Progressive, uniaxial step-wise compressive strains of 0%, 2%, 4%, 8% and 12% were applied to each specimen at a strain rate of $0.01s^{-1}$ using a custom testing device (See Figure 5). Each sample was μCT imaged initially and after the application of each strain step to visualize the

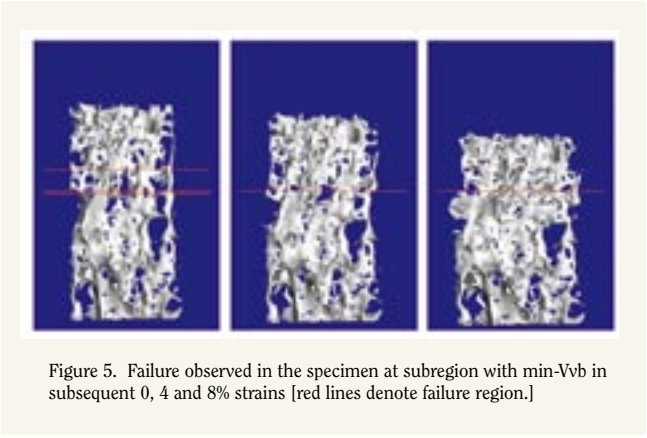

Figure 5. Failure observed in the specimen at subregion with min-Vvb in subsequent 0, 4 and 8% strains [red lines denote failure region.]

location of progressive deformation of trabeculae throughout the specimen. The modulus was determined from the slope fit to the linear portion of the composite step-wise stress-strain data. The yield stress was determined at the point where the stress-strain data became non-linear using 0.2% strain offset. Regression models were fit (Levenberg-Marquardt method) to the function: σY, $E = a \cdot \rho_{tiss} \cdot (Vv_b)^2 + b$.

The average bone tissue densities for cancer and non-cancer specimens were 1.66 ±0.32 and 1.82 ± 0.31 g/cc respectively (statistically not significant, p=0.40). For all specimens, serial μCT images demonstrated that failure occurred predominantly at the transaxial sub-region that exhibited the minimum-Vv_b. For both the cancer (CA) and non-cancer (NC) specimens the sub-region with the minimum-Vv_b accounted for more of the variability in the measured mechanical properties than the average Vv_b for the entire specimen (See Table 4).

The results of this study validate the application of

Table 4. Coefficients of var. (r^2) values for σ_Y, $E = a \times \rho_{tiss} \times (Vv_b)^2 + b$ model.

Specimen	Indep.		Ys			E	
Type	Var.	R^2	a	b	R^2	a	b
CA	avg- Vvb	0.81	0.161	5.10E-04	0.81	4.36	0.072
CA	min-Vvb	0.92	17.1	1.50E-03	0.88	451.2	0.103
CA+NC	avg- Vvb	0.63	0.002	3.04E+00	0.62	0.085	140.2
CA+NC	min-Vvb	0.66	0.003	3.24E+00	0.65	0.65	147.6

power law functions of bone tissue density and bone volume fraction to derive the strength and modulus of pathologic bone tissue. The constitutive relationships for metastatic cancer bone tissue and non-cancer bone are similar and can be approximated statistically by a single power law function with Vv_b and ρ_{tiss} as independent explanatory variables that model trabecular bone as a rigid porous foam. Therefore, the weakest portion of the specimen, not the average properties of the specimen, governed the mechanical behavior of these pathologic bone specimens.

Prediction of Pathologic Bone Fracture Using CT Structural Rigidity Analysis

We previously demonstrated that structural rigidity analysis of transaxial quantitative CT images accurately predicted failure load of vertebrae with simulated osteolytic defects *ex-vivo*. [43] Since the spine is the most frequent site of skeletal metastases in breast cancer patients,[44] the aim of this work was to prove that structural rigidity analysis of transaxial CT image data *in-vivo* predicts fracture of cancer patients with spinal metastases better than current clinical and radiographic guidelines.

We prospectively evaluated the fracture risk of 106 women with metastatic breast cancer to the spine. The *in-vivo* load carrying capacity of vertebrae with metastatic breast cancer was estimated non-invasively using our QCT based algorithm. The loads applied to affected thoracic and lumbar vertebrae during typical activities of daily living such as bending over to lift a 10 kg mass or arising from a chair were estimated using our optimization based model for spinal loading that takes into account the load bearing capacity of the thoracic cage. The quotient of the load applied to the affected vertebra divided by the load carrying capacity of the vertebra provides an index for assessing fracture risk during this specific activity. This fracture risk index (FRI), was calculated for each vertebrae between T8-L5 using two different load scenarios for each patient: a) lifting a 10 kg mass and b) arising from a chair. FRI>1 implies that fracture would occur during the applied load condition. We compared the accuracy of FRI to the best available clinical and radiographic criteria for predicting metastatic spine fracture to test the hypothesis that structural rigidity assessed by algorithms based on CT measurements predicted the failure load of a vertebra containing a defect better than current radiographic methods.

CT scans were performed on all patients to provide the data to calculate the load capacity (failure load) of the vertebrae.[45] Axial and bending rigidities were calculated relative to the modulus-weighted centroid, as in all previous experiments.The load carrying capacity of each vertebra was calculated using a two-dimensional plane strain model for the vertebra loaded in combined axial compression and forward bending. The yield load for this scenario was calculated from the cross-sectional geometric and material properties of the vertebra:

$$\varepsilon = F_z / EA + M_y \, c / EI$$

where ε, the strain at failure = 1% (since at the material level bone fails in compression at a constant strain of 1% independent of density),[39] c=distance from neutral axis to the outermost point in the AP direction, and $M_y = F_z \, x$, where x = distance from the neutral axis to the point of load application

at the center of the vertebral body. The applied load at each vertebra for simple lifting tasks was calculated using an optimization-based model that accounted for the subject's height and weight.

There are few radiographic guidelines for predicting vertebral fracture. Most guidelines based on plain radiographs of the spine in the frontal and sagittal projections are used to predict spinal instability and risk for neurological injury *after* the fracture has already occurred. The CT based method described by Taneichi *et al.*[46] to predict vertebral fracture risk, as a function of the size and location of the defect alone, was the best radiographic method reported in the literature. Four factors were combined to assess fracture risk: percentage of tumor occupancy in the vertebral body, destruction of the pedicle, destruction of the posterior elements except the pedicle, and destruction of the costovertebral joint. Fracture risk was defined as predicted probability>0.5.

To assess the accuracy of the two methods for predicting vertebral fracture, it was necessary to determine if a vertebral fracture occurred in the study subjects. Metastatic lesions are constantly changing in size, shape and the bone tissue forming the lesion. Therefore any method that predicts fracture risk for skeletal metastases is valid for only a finite period of time. Vertebral fracture occurrence was determined over a four-month surveillance period. We were blinded to the patients' clinical course or treatment regimen. Patients with previous spine fractures were eliminated from the analysis so as not to positively bias our results.

Vertebral fracture occurrence was defined by commonly used criteria for osteoporotic vertebral fracture.[47] Vertebral heights were measured on all subjects from plain radiographs and/or MRI scans that included part or all of the spinal column. Wedge fractures were diagnosed if there was a 15% loss of height from one side of the vertebrae compared to the other in either the frontal or sagittal planes. Axial compression fractures were diagnosed if there was a 15% loss of vertebral height compared to adjacent vertebrae. An independent observer, unaware of the fracture risk predictions of the subjects, reviewed all plain radiographs and MRI scans.

The CT based structural rigidity analysis and CT based analysis of lesion size and location using Taneichi guidelines[46] for assessing fracture risk were compared using clinical data from breast cancer patients with spinal metastases. Of the 106 patients, ten patients suffered one or more new vertebral fracture over the 4-month observation period. Both the CT based structural rigidity analysis and the Taneichi criteria predicted that these 10 patients were at increased fracture risk (sensitivity = 100% for either method). However, the CT rigidity analysis was better at predicting which patients would *not* fracture an affected vertebra (specificity=49% when FRI>1 for lifting a 10 kg mass) compared to the Taneichi CT criteria (specificity=20%). Instead of calculating the FRI for lifting a 10 kg mass, if the load carrying capacity of the vertebra was normalized by the patient's body mass index and the threshold for predicting vertebral fracture set to achieve 100% sensitivity, the specificity for predicting no vertebral fracture was improved to 69%. Using logistic regression analysis, the estimated relative risk for fracture based on FRI>1 was RR=4.2 (95% confidence interval: 1.4 – 12.8, $p<0.001$). When controlling for BMI in the model, the adjusted relative risk for fracture based on FRI>1 is RR=7.9 (95% confidence interval: 1.8 – 34.5, $p<0.001$).

We have developed a non-invasive method using transaxial CT images of the torso which are attained routinely in breast cancer patients for surveillance of liver metastases and demonstrated that these same images can be used successfully to predict the risk of vertebral fracture in those patients with metastases to the spine.

The analytic model estimates the load applied to each vertebra for specific loading cases. Many of the patients enrolled in our study were instructed by their oncologists to refrain from strenuous activities that might put them at increased risk for vertebral fracture. Patients abstaining from activities such as heavy lifting negatively bias our analysis and decrease the number of vertebral fractures since fewer patients engaged in the index activity that we simulated. This is in comparison to our study of children with benign tumors of the appendicular skeleton where the predicted fracture risk using CT based structural analysis was 100% sensitive and 94% specific. None of these children were aware of the presence of the tumor and they did nothing to alter their physical activities. In the future it may be useful to patients and their physicians to provide a list of activities that result in FRI ≥ 1 and FRI < 1. By normalizing the load carrying capacity of the vertebra by the patient's body mass index, the specificity improved significantly to 69% compared to the 49% specificity for FRI ≥ 1 when lifting a 10 kg mass. The advantage of this empiric approach is that it makes no assumption as to the patient's level of activity and accounts for the patient's height and weight, which likely affect the risk of pathologic fracture. In conclusion, CT based structural rigidity analysis was as sensitive but significantly more specific than the best radiographic guidelines for estimating metastatic cancer vertebral fracture risk.

References

1. Michaeli, D.A., et al., *Density predicts the activity-dependent failure load of proximal femora with defects.* Skeletal Radiol, 1999. **28**(2): p. 90-5.
2. Fidler, M., *Incidence of fracture through metastases in long bones.* Acta Orthop Scand, 1981. **52**(6): p. 623-7.
3. Gitelis, S., R. Wilkins, and E.U. Conrad, 2nd, *Benign bone tumors.* Instr Course Lect, 1996. **45**: p. 425-46.
4. Garmatis, C.J. and F.C. Chu, *The effectiveness of radiation therapy in the treatment of bone metastases from breast cancer.* Radiology, 1978. **126**(1): p. 235-7.
5. Scheid, V., et al., Clinical course of breast cancer patients with osseous metastasis treated with combination chemotherapy. Cancer, 1986. **58**(12): p. 2589-93.
6. Rizzoli, R., *et al., Effects of oral clodronate on bone mineral density in patients with relapsing breast cancer.* Bone, 1996. **18**(6): p. 531-7.
7. Cobleigh, M.A., *Hormone replacement therapy and nonhormonal control of menopausal symptoms in breast cancer survivors.* Cancer Treat Res, 1998. **94**: p. 209-30.
8. Theriault, R.L. and G.N. Hortobagyi, *The evolving role of bisphosphonates.* Semin Oncol, 2001. **28**(3): p. 284-90.
9. Boissier, S., et al., Bisphosphonates inhibit breast and prostate carcinoma cell invasion, an early event in the formation of bone metastases. Cancer Res, 2000. 60(11): p. 2949-54.
10. Harrington, K.D., Orthopaedic management of extremity and pelvic lesions. Clin Orthop, 1995(312): p. 136-47.
11. Love, R.R., Tamoxifen in axillary node--negative breast cancer: multisystem benefits and risks. Cancer Invest, 1992. 10(6): p. 587-93.
12. Tanaka, M., *et al., Sclerosis of lytic metastatic bone lesions during treatment with pamidronate in a patient with adenocarcinoma of unknown primary site.* Eur Spine J, 1996. **5**(3): p. 198-200.
13. Schocker, J.D. and L.W. Brady, *Radiation therapy for bone metastasis.* Clin Orthop, 1982(169): p. 38-43.
14. Snyder, B., Hecht AC, Tedrow JR, Hauser DL. *Structural rigidity measured by CT accurately predicts fracture in children with benign tumors of the appendicular skeleton. in 45th Annual Meeting of the Orthopedic Research Society.* 2000. Orlando, FL.
15. Houston, S.J. and R.D. Rubens, *The systemic treatment of bone metastases.* Clin Orthop, 1995(312): p. 95-104.
16. Jemal, A., et al., Cancer statistics, 2003. CA Cancer J Clin, 2003. **53**(1): p. 5-26.
17. Hortobagyi, G.N., *et al., Long-term prevention of skeletal complications of metastatic breast cancer with pamidronate. Protocol 19 Aredia Breast Cancer Study Group.* J Clin Oncol, 1998. **16**(6): p. 2038-44.
18. Hortobagyi, G.N., *The status of breast cancer management: challenges and opportunities.* Breast Cancer Res Treat, 2002. **75 Suppl 1**: p. S61-5; discussion S57-9.
19. Hoskin, P., *Radiotherapy, in Tumor Bone Diseases and Osteoporosis in Cancer Patients,* J. Body, Editor. 2000, Marcel Dekker, Inc.: New York. p. 263-286.
20. Coleman, R.E., *Metastatic bone disease: clinical features, pathophysiology and treatment strategies.* Cancer Treat Rev, 2001. 27(3): p. 165-76.
21. Perez, E.A., *Metastatic bone disease in breast cancer: the patient's perspective.* Semin Oncol, 2001. **28**(4 Suppl 11): p. 60-3.
22. Pritchard, K.I., *Hormone replacement in women with a history of breast cancer.* Oncologist, 2001. **6**(4): p. 353-62.
23. Van Poznak, C., *How are bisphosphonates used today in breast cancer clinical practice?* Semin Oncol, 2001. **28**(4 Suppl 11): p. 69-74.
24. Beals, R., Lawton, G, Snell, W, *Prophylactic internal fixation of the femur in metastatic breast cancer.* Cancer, 1971. **28**: p. 1350-4.
25. Bunting, R.e.a., *Pathologic fracture risk in rehabilitation of patients with bony metastases.* Clinical Orthopaedics and Related Research, 1985. **192**: p. 222-7.
26. Cheng, D., Seitz, C, Eyre, H, *Nonoperative management of femoral, humeral, and acetabular metastases in patients with breast carcinoma.* Cancer, 1980. **45**: p. 1533-7.
27. Harrington, K.D., *New trends in management of lower extremity metastases.* Clinical Orthopaedics, 1982. **169**: p. 53-61.
28. Hayes, W.C., S.J. Piazza, and P.K. Zysset, *Biomechanics of fracture risk prediction of the hip and spine by quantitative computed tomography.* Radiol Clin North Am, 1991. **29**(1): p. 1-18.
29. Hulley, S., Cummings, S, *Designing Clinical Research: An Epidemiologic Approach.* 1988, Baltimore: Williams and Wilkins.
30. Eilkins, R., Sim, F, Springfield, D, *Metastatic disease of the femur.* Orthopaedics, 1992. **15**: p. 621-30.
31. Parrish, F., Murray, J, *Surgical treatment for secondary neoplastic fractures. A retrospective study of 96 patients.* Journal of Bone and Joint Surgery, 1970. **52A**: p. 665-86.
32. Thompson, R., *Impending fracture associated with bone destruction.* Orthopaedics, 1992. **15**: p. 547-50.
33. Keene, J., *et al., Metastatic breast cancer in the femur: A search for the lesion at risk of fracture.* Clinical Orthopaedics and Related Research, 1986. **203**: p. 282-88.
34. von Stechow D, N.A., Cordio MA, Mueller R, Snyder BD, *Biomechanical Behavior of Skeletal Metastases.* Oncology, 2003. **17**(4(S3)): p. 28.
35. Mirels, H., *Metastatic disease in long bones.* Clinical Orthopaedics, 1989: p. 256-64.
36. Windhagen, H.J., et al., *Predicting failure of thoracic vertebrae with simulated and actual metastatic defects.* Clinical Orthopaedics and Related Research, 1997. **344**: p. 313-319.
37. Rice, J.C., S.C. Cowin, and J.A. Bowman, *On the dependence of the elasticity and strength of cancellous bone on apparent density.* J Biomech, 1988. **21**(2): p. 155-68.
38. Snyder, S.M. and E. Schneider, *Estimation of mechanical properties of cortical bone by computed tomography.* Journal of Orthopaedic Research, 1991. **9**: p. 422-431.
39. Keaveny, T.M., *et al., Differences between the tensile and compressive strengths of bovine tibial trabecular bone depend on modulus.* J Biomech, 1994. **27**(9): p. 1137-46.
40. Gibson LJ, A.M., *Cellular Solids.* 1997: Cambridge University Press.
41. Copley, L. and J.P. Dormans, *Benign pediatric bone tumors. Evaluation and treatment.* Pediatr Clin North Am, 1996. **43**(4): p. 949-66.
42. Hecht, A.C. and M.C. Gebhardt, *Diagnosis and treatment of unicameral and aneurysmal bone cysts in children.* Curr Opin Pediatr, 1998. **10**(1): p. 87-94.
43. Honore, P., *et al., Osteoprotegerin blocks bone cancer-induced skeletal destruction, skeletal pain and pain-related neurochemical reorganization of the spinal cord.* Nat Med, 2000. **6**(5): p. 521-8.
44. Tubiana-Hulin, M., **Incidence, prevalence and distribution of bone metastases.** Bone, 1991. **12**(Suppl 1): p. S9-10.
45. Whealan, K.M., et al., *Noninvasive imaging predicts failure load of the spine with simulated osteolytic defects.* J Bone Joint Surg Am, 2000. **82**(9): p. 1240-51.
46. Taneichi, H., et al., *Risk factors and probability of vertebral body collapse in metastases of the thoracic and lumbar spine.* Spine, 1997. **22**(3): p. 239-45.
47. Genant, H.K., et al., *Vertebral fracture assessment using a semiquantitative technique.* J Bone Miner Res, 1993. **8**(9): p. 1137-48.